Genes & Diseases (2024) 11, 430–448

Available online at www.sciencedirect.com

ScienceDirect

journal homepage: www.keaipublishing.com/en/journals/genes-diseases

FULL LENGTH ARTICLE

Zinc finger protein 831 promotes apoptosis and enhances chemosensitivity in breast cancer by acting as a novel transcriptional repressor targeting the *STAT3/Bcl2* signaling pathway

Jun Fan [a], Zhe Zhang [a], Hongqiang Chen [b,c], Dongjiao Chen [b,d], Wenbo Yuan [b,e], Jingzhi Li [b,e], Yong Zeng [b,c], Shimeng Zhou [b,f], Shu Zhang [a], Gang Zhang [a], Jiashen Xiong [a], Lu Zhou [a], Jing Xu [a], Wenbin Liu [b,c,*], Yan Xu [a,*]

[a] *Department of Breast and Thyroid Surgery, Daping Hospital, Army Medical University (Third Military Medical University), Chongqing 400042, China*
[b] *Institute of Toxicology, College of Preventive Medicine, Army Medical University (Third Military Medical University), Chongqing 400038, China*
[c] *Department of Environmental Health, College of Preventive Medicine, Army Medical University (Third Military Medical University), Chongqing 400038, China*
[d] *Anesthesia and Intensive Care, Chinese University of Hong Kong, Hong Kong SAR 999077, China*
[e] *School of Public Health, Xinxiang Medical University, Xinxiang, Henan 453003, China*
[f] *School of Public Health, China Medical University, Shenyang, Liaoning 110122, China*

Received 21 February 2022; received in revised form 18 November 2022; accepted 27 November 2022
Available online 29 December 2022

KEYWORDS
Apoptosis;
Breast cancer;
Chemosensitivity;
STAT3;
ZNF831

Abstract Emerging evidence suggested that *zinc finger protein 831* (*ZNF831*) was associated with immune activity and stem cell regulation in breast cancer. Whereas, the roles and molecular mechanisms of *ZNF831* in oncogenesis remain unclear. *ZNF831* expression was significantly diminished in breast cancer which was associated with promoter CpG methylation but not mutation. Ectopic over-expression of *ZNF831* suppressed breast cancer cell proliferation and colony formation and promoted apoptosis *in vitro*, while knockdown of *ZNF831* resulted in an opposite phenotype. Anti-proliferation effect of *ZNF831* was verified *in vivo*. Bioinformatic

* Corresponding author.
E-mail addresses: liuwenbin@tmmu.edu.cn (W. Liu), xy931@163.com (Y. Xu).
Peer review under responsibility of Chongqing Medical University.

https://doi.org/10.1016/j.gendis.2022.11.023

analysis of public databases and transcriptome sequencing both showed that *ZNF831* could enhance apoptosis through transcriptional regulation of the *JAK/STAT* pathway. ChIP and luciferase report assays demonstrated that ZNF831 could directly bind to one specific region of *STAT3* promoter and induce the transcriptional inhibition of *STAT3*. As a result, the attenuation of *STAT3* led to a restraint of the transcription of *Bcl2* and thus accelerated the apoptotic progression. Augmentation of *STAT3* diminished the apoptosis-promoting effect of *ZNF831* in breast cancer cell lines. Furthermore, *ZNF831* could ameliorate the anti-proliferation effect of capecitabine and gemcitabine in breast cancer cell lines. Our findings demonstrate for the first time that *ZNF831* is a novel transcriptional suppressor through inhibiting the expression of *STAT3*/*Bcl2* and promoting the apoptosis process in breast cancer, suggesting *ZNF831* as a novel biomarker and potential therapeutic target for breast cancer patients.

Abbreviations

BLCA	bladder urothelial carcinoma
BRCA	breast carcinoma or breast cancer
Cape	capecitabine
ChIP	chromatin immunoprecipitation
CI	confidence interval
COAD	colon adenocarcinoma
ER	estrogen receptor
FDR	false discovery rate
GAPDH	glyceraldehyde-3-phosphate dehydrogenase
GBM	glioblastoma multiforme
GEM	gemcitabine
GO	gene ontology
GSEA	gene set enrichment analysis
HER2	human epidermal growth factor receptor
KEGG	Kyoto Encyclopedia of Genes and Genomes
MLD BRCA	mixed lobular and ductal breast carcinoma
m6A	N6-methyladenosine
PR	progesterone receptor
qRT-PCR	real-time quantitative polymerase chain reaction
sCNA	DNA copy-number alterations
STAT3	*signal transducer and activator of transcription 3*
TCGA	the Cancer Genome Atlas
ZNFs	zinc finger proteins
ZNF831	*zinc finger protein 831*

Introduction

Breast cancer (BRCA) keeps up the leading cancer-related cause of disease in women.[1] With an estimated 2.3 million new patients (11.7%), BRCA has exceeded lung cancer (11.4%) as the most commonly diagnosed cancer in the world.[2] Numerous risk factors played vital roles in BRCA progression, including genetic predisposition, exposure to specific environmental factors, microbiome, and immune microenvironment.[3,4] Not only considerable mortality could be caused by lung, bone, brain, and liver metastases,[5–8] but also the poor prognosis is partially attributed to chemoresistance and anti-apoptosis responses of the cancer cells.[9] Even though much epidemiological and clinical research has been conducted for years, more mechanisms of BRCA oncogenesis about apoptosis and chemoresistance remain to be explored. Therefore, identifying novel biomarkers associated with the apoptotic process and chemosensitivity and exploring their molecular mechanism would be meaningful and crucial for early diagnosis and targeting therapy among BRCA patients.

Zinc finger proteins (ZNFs) belong to the largest transcription factor family and the zinc finger motifs have been revealed to possess interacting abilities with DNA, RNA, proteins, and lipids.[10–13] Up to now, a total of 8 different classes of zinc finger motifs have been reported, including Cys2His2-like, Gag knuckle, Treble clef, Zinc ribbon, Zn2/Cys6, TAZ2 domain-like, Zinc binding loops, and Metallothionein.[14–21] With different combinations of multiple zinc finger motifs, ZNFs may greatly expand their diverse roles in gene regulation under different cell contexts or stimulations. Generally, they are characterized by classic zinc finger motifs and can activate or repress the transcription level of target genes by binding to gene promoters.[22] Moreover, one member of ZNFs may display its functions on transcriptional regulation toward thousands of downstream genes owing to the same or similar promoter binding sites. As a result, ZNFs exert significant differential biological functions and hence influence carcinogenesis and progression, including proliferation, migration, invasion, stemness, apoptosis, cell cycle, senescence, autophagy, *etc*.[23–29] Studies about how ZNFs influence and participate in BRCA oncogenesis outbursts and come to the top in the last decade. Many members of ZNFs were exposed and explored. *Zinc finger protein 831* (*ZNF831*) is one of them and its transcription product locates in the cytoplasm. Recent evidence has indicated that *ZNF831* was involved both in immune regulation[30,31] and preeclampsia.[32] It also

has been reported that *ZNF831* was negatively correlated with stem cell phenotype and reduced the relapse risk of BRCA.[30] This evidence suggested that *ZNF831* may play a pivotal role in BRCA tumorigenesis and progression. Up to now, the role and molecular mechanism of *ZNF831* in BRCA oncogenesis remain unclear.

In this study, we investigated the expression regulation, biological function, molecular mechanism, and clinical significance of *ZNF831* gene in breast cancer. We found that *ZNF831* expression down-regulation was mainly regulated by promoter methylation but not a genetic alteration in breast cancer. *ZNF831* expression inhibited tumorigenesis in breast cancer *in vitro* and *in vivo*. Mechanistically, *ZNF831* promoted BRCA apoptosis via transcriptionally repressing *signal transducer and activator of transcription 3* (*STAT3*) and subsequently inhibiting *Bcl2*. *ZNF831* enhanced chemosensitivity to capecitabine and gemcitabine in BRCA. Our study demonstrated for the first that *ZNF831* gene acted as a novel tumor suppressor by regulating the *STAT3*/*Bcl2* signaling axis in BRCA, hoping these results could contribute to BRCA tumorigenesis exploration and lay the foundation for early diagnosis and targeted therapy.

Materials and methods

Bioinformatics analysis

The transcription level of *ZNF831* was analyzed through several public databases, including TIMER 2.0 (http://timer.cistrome.org/), TCGA (https://www.cancer.gov/), and Oncomine (https://software.oncomine.com/). In detail, the TIMER 2.0 database was conducted to compare the expression of *ZNF831* between tumor and adjacent normal tissues in pan-cancer by the "Gene" module. Besides, we also performed the transcriptional differences of *ZNF831* between tumor and adjacent normal samples among the TCGA-BRCA cohort and the Oncomine cohorts. Furthermore, *ZNF831* protein expression was searched from the Human Protein Atlas (HPA, https://www.proteinatlas.org/) database. DNA methylation data of *ZNF831* was analyzed through probe-level methylation and CpG-aggregated methylation modules of the SMART. Genetic alterations of *ZNF831* were explored in the cBioPortal through breast invasive carcinoma. LinkedOmics was used for *ZNF831* correlated gene analysis. GSEA 4.0.3 from GSEA was used to analyze 20,530 genes in the TCGA genomic matrix grouped by the median *ZNF831* expression level.

Cell culture

MDA-MB-231 and MCF-7 cells were cultured in Dulbecco's Modified Eagle Medium/High-glucose medium (HyClone, USA) containing 10% fetal bovine serum (FBS, HyClone, USA) at 5% CO_2 and 37 °C. BT474 and HCC38 cells were cultured in Roswell Park Memorial Institute-1640 medium (HyClone, USA) containing 10% fetal bovine serum (HyClone, USA) at 5% CO_2 and 37 °C. All cells were procured directly from the American Type Culture Collection. Decitabine (5-Aza-2′-deoxycytidine) was supplied as a powder (Abcam, UK) and dissolved in DMSO at a final concentration of 10 μM.

Tissues samples

The study cohort contained 14 pairs of specimens including paired adjacent tissues and BRCA tissues. All tissues were obtained from the Daping Hospital of Army Medical University (Chongqing, China). Prior patient consent and approval from the Ethics Committee of Daping Hospital were obtained. Patients treated with radiotherapy/chemotherapy before surgery were excluded from this study.

Plasmid transfection

ZNF831 over-expression associated plasmids (Pcdna3.1-3xFLAG and Pcdna3.1-*ZNF831*-3xFLAG), *ZNF831* knockdown associated plasmids (pLVx-mCherry-T2A-puro and pLVx-*ZNF831*-shRNA-mCherry-T2A-puro) and *STAT3* over-expression associated plasmids (pLVX-Puro-FLAG and pLVX-Puro-*STAT3*-FLAG) were constructed and purchased for transfection (Leqin Corporation). The primer sequences for constructing the plasmid were listed in Table S1. Transient and stable transfection was performed by ViaFect (Promega, USA) following the manufacturer's instructions.

Cell viability assay

Cells were seeded into 96-well plates 24 h ahead and were transiently transfected for 48 h. Cell proliferation was determined by the CellTiter 96 AQueous One Solution Cell Proliferation Assay system (Promega, USA) according to the manufacturer's instructions. After 1 h incubation in a humidified atmosphere (5% CO_2, 37 °C), absorbance at 490 nm was measured every 24 h using a SpectraMax i3 microplate reader (Molecular Devices, USA).

Colony formation assay

Cells were seeded into 6-well plates. After 2 weeks of incubation in a humidified atmosphere (5% CO_2, 37 °C), the colonies were fixed with 4% paraformaldehyde (Solarbio) for 20 min and stained with crystal violet (Solarbio) at room temperature. Cell colonies were imaged and the number of colonies with >50 cells was counted.

Cell apoptosis assay

Cells were seeded into 6-well plates 24 h ahead and were transiently transfected for 48 h. Cell apoptosis was analyzed using the Annexin V-APC/7-AAD (7-amino-actinomycin D) Apoptosis Detection Kit (KeyGEN, China) according to the manufacturer's instructions. The cell apoptosis data were analyzed by FlowJo 7.6.1 software (Tree Star, USA).

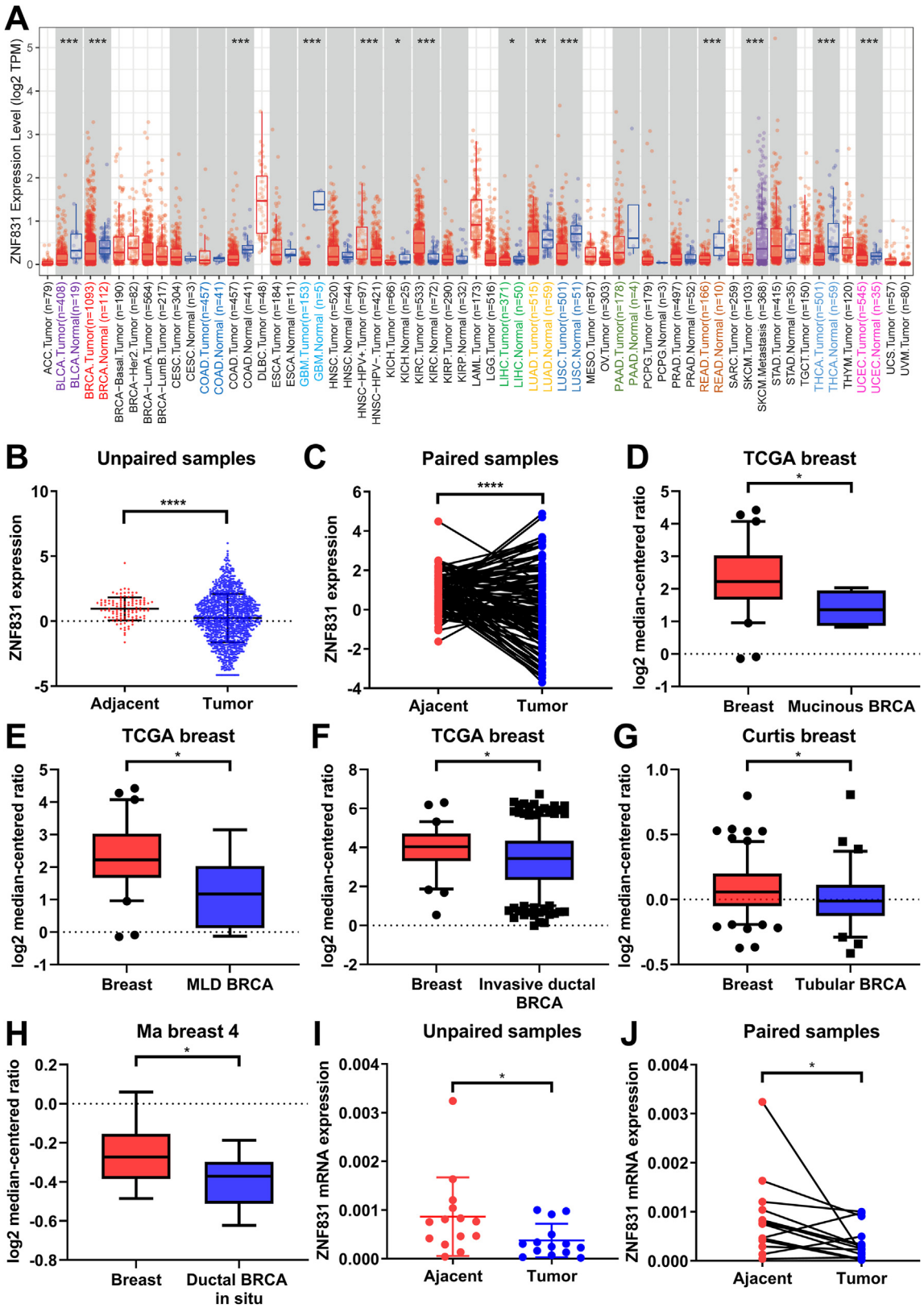

Figure 1 *ZNF831* is down-regulated in most cancer types and BRCA patients. **(A)** The differential expression between tumor and adjacent normal tissues for *ZNF831* across all TCGA tumor types. The data was processed by the TIMER2.0 web server and presented as the means ± SEM (the Wilcoxon test). **(B, C)** *ZNF831* mRNA level is diminished in BRCA tissue *vs*. (B) unpaired normal breast tissue and (C) adjacent paired normal breast tissue. The data was from the BRCA data set of the TCGA cohort (*t*-test). **(D–H)** The expression of *ZNF831* between the normal breast tissue and (D) mucinous BRCA in TCGA breast research, (E) MLD BRCA in TCGA

qRT-PCR

RNA was extracted using RNAiso Plus (TaKaRa, Japan) according to the manufacturer's instructions, and then reverse transcription was performed by the GoScript reverse transcriptional system (Promega, USA). The RNA expression level was determined using the GoTaq qPCR Master Mix (Promega, USA) on the Bio-Rad Real-Time PCR System (Bio-Rad, USA). Sequences of primers for quantitative real-time polymerase chain reaction (qRT-PCR) in this study are listed in Table S2.

Western blot analysis

The protein of the cells was obtained for Western blot analysis. Cells were collected to homogenize in ice with RIPA buffer solution (Solarbio, China) for protein extraction. The 0.5 M EDTA (pH 8.0) (Solarbio, China), protein phosphatase inhibitor mixture (Solarbio, China), and deacetylase inhibitor mixture (Solarbio, China) were added for cell lysis. The concentration of protein was measured by a BCA protein assay kit (CWBIO, China). 12% SDS-PAGE was selected for electrophoresis and the proteins were transferred onto the PVDF membrane. The membrane was incubated with 3% BSA at room temperature for 1 h. The primary antibody was then incubated at the appropriate concentration over night at 4 °C. The antibodies used in this study were as follows: STAT3 (1:1000, Proteintech), P-STAT3 (Tyr705) (1:1000, Beyoime), Bcl2 (1:1000, Proteintech), Bax (1:1000, Proteintech), GAPDH (1:1000, CWBIO). Secondary antibodies conjugated with horseradish peroxidase were used for further incubation for 2 h at room temperature and visualized using ECLTM Western Blotting Detection Reagent (Bio-Rad, USA).

Chromatin immunoprecipitation (ChIP) assay

ChIP analysis was performed on transiently transfected BRCA cells with ectopic over-expressed *ZNF831* using the SimpleChIP Enzymatic Chromatin IP Kit (Magnetic Beads) (CST, USA) according to the manufacturer's instructions. DYKDDDDK Tag (D6W5B) Rabbit mAb (binds to the same epitope as Sigma's Anti-FLAG M2 Antibody (CST, USA) was used to drag FLAG. Sequences of primers for promoter region in this study are listed in Table S3.

Luciferase reporter assay

Cells were seeded in 24-well plates and human *STAT3* promoter (−2000 to +200) luciferase reporter plasmid was transiently transfected with *ZNF831* expression plasmids into cells. Renilla luciferase pRL-SV40 (Promega) was used to normalize the luciferase activity, which was further measured using the dual-luciferase reporter assay system (Promega).

Chemosensitivity assay

Chemotherapeutic drugs were purchased and a cell viability assay was conducted to evaluate the function of *ZNF831* in chemosensitivity. The final concentration for capecitabine (RO 09-1978) (Selleck, USA) was 1000 μM for all, and gemcitabine (LY-188011) (Selleck, USA) was 500 μM for MDA-MB-231, BT474, and HCC38, and 1000 μM for MCF-7.

Cell-line-derived xenograft model

All procedures were approved by the Laboratory Animal Welfare and Ethics Committee of the Third Military Medical University and carried out in strict compliance with the relevant guidelines. Six-week-old female BALB/C nude mice were randomly assigned to the vehicle and over-expression groups. Induction of tumor xenografts was performed by subcutaneous injection of 0.1 mL cell suspensions containing 5×10^6 cells in the logarithmic phase into the right flank of the animal. Tumor length (*L*) and width (W) were measured via vernier caliper twice a week, and the volume was calculated based on the following equation: $V = L \times W^2/2$. After one month, the mice were killed and the tumors were aseptically excised and weighed up. Tumor fragments were used for pathological analysis and IHC.

Statistical analysis

All statistical analyses were performed using SPSS 26.0 software (SPSS, Inc., Chicago, IL, USA). All data were presented as the mean ± standard deviation (SD) of at least three independent experiments. Student's *t*-test was used to analyze the significance of differences between the two groups. Wilcoxon test was used to analyze the significance of differential expression between tumor and adjacent normal tissues for *ZNF831* across all TCGA tumor types. Pearson correlation test was selected as correlation analysis in LinkedOmics. $P < 0.05$ was considered statistically significant.

Results

ZNF831 is down-regulated in most cancer types and BRCA patients

To briefly explore the spectrum of *ZNF831* expression across most human cancer types, we first analyzed the transcription level of *ZNF831* through the TIMER 2.0 database. Results showed that *ZNF831* was significantly down-regulated in many kinds of cancers, including bladder urothelial

breast research, (F) invasive ductal BRCA in TCGA breast research, (G) tubular BRCA in Curtis breast research, and (H) ductal BRCA *in situ* in Ma breast 4 research. The data was from the BRCA data set of the Oncomine database (*t*-test). **(I, J)** *ZNF831* mRNA expression level in BRCA tissue *vs.* (I) unpaired normal breast tissue and (J) adjacent paired normal breast tissue. The data was from clinical BRCA tissue samples (*t*-test). BRCA, breast carcinoma or breast cancer; MLD BRCA, mixed lobular and ductal breast carcinoma; qRT-PCR: real-time quantitative polymerase chain reaction. *$P < 0.05$, **$P < 0.01$, ***$P < 0.001$, ****$P < 0.0001$.

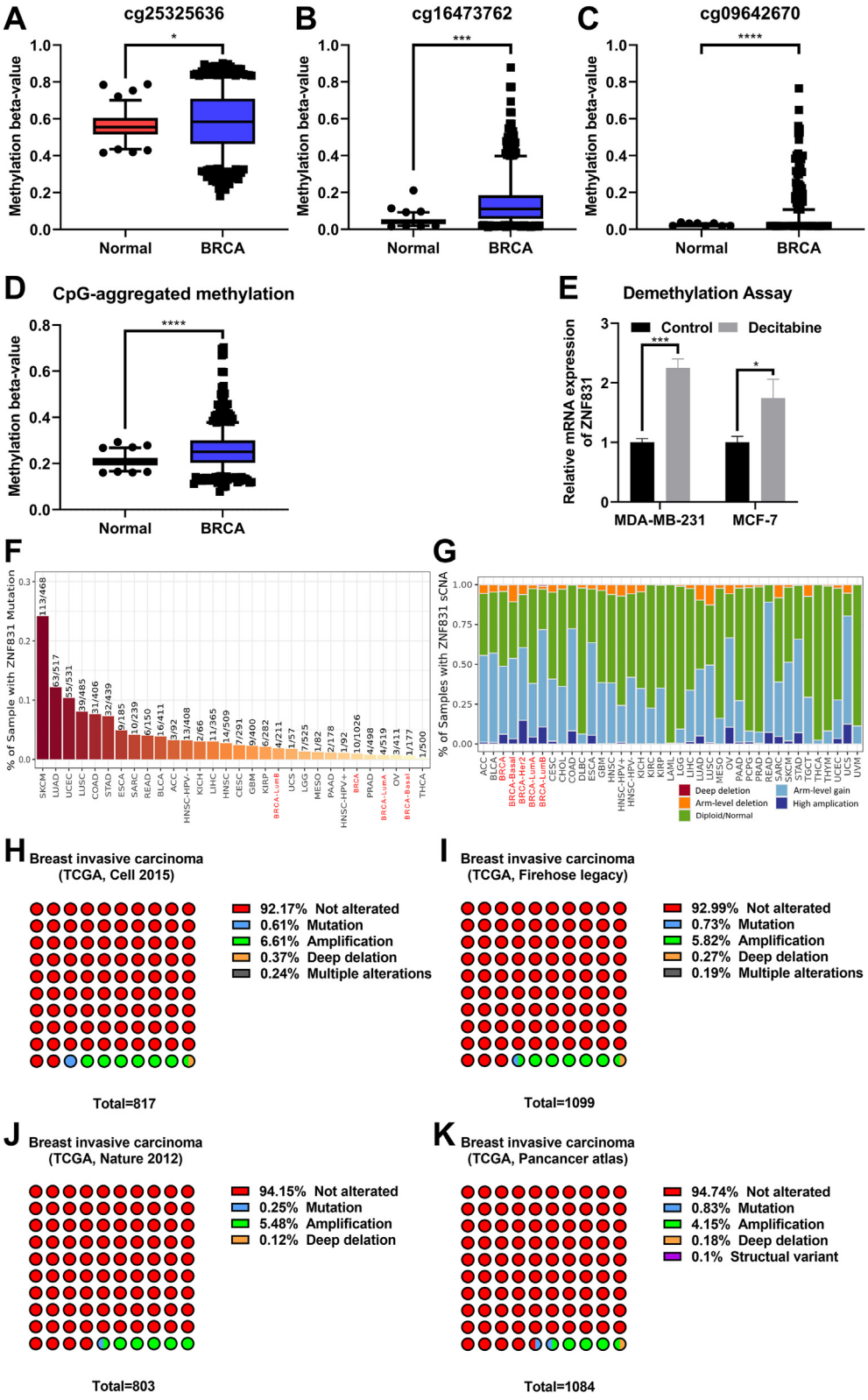

Figure 2 Down-regulation of *ZNF831* correlates with its promoter hypermethylation in BRCA samples. **(A)** The cg25325636 site methylation value in BRCA between normal and tumor. **(B)** The cg16473762 site methylation value in BRCA between normal and tumor. **(C)** The cg09642670 site methylation value in BRCA between normal and tumor. **(D)** The aggregation of cg25325636, cg16473762, and cg09642670 site methylation values in BRCA between normal and tumor. **(E)** The expression of *ZNF831* was measured by qRT-PCR in MDA-MB-231 and MCF-7 after demethylation treatment. **(F)** Somatic mutation frequency of *ZNF831* for each TCGA cancer type. **(G)** The relative proportion of different sCNA states of the *ZNF831* for all TCGA cancer types. **(H—K)**

carcinoma (BLCA) ($P < 0.001$), breast invasive carcinoma (BRCA) ($P < 0.001$), colon adenocarcinoma (COAD) ($P < 0.001$), glioblastoma multiforme (GBM) ($P < 0.001$), *etc* (Fig. 1A). In addition, we verified the results of BRCA in unpaired ($P < 0.0001$) (Fig. 1B) and paired ($P < 0.0001$) (Fig. 1C) samples from TCGA-BRCA cohort. Furthermore, the result was enhanced again by 5 independent cohort studies for different BRCA subtypes from the Oncomine database ($P < 0.05$) (Fig. 1D–H). These findings were verified by qRT-PCR analysis of *ZNF831* mRNA expression from 10 pairs of normal and BRCA samples in unpaired ($P < 0.05$) and paired ($P < 0.05$) ways (Fig. 1I, J). The expression difference in protein level was verified in immunohistochemistry from the HPA database and the results suggested that ZNF831 was localized in the cytoplasm and expressed poorly in BRCA tissues (Fig. S1A, B).

Down-regulation of *ZNF831* correlates with its promoter hypermethylation in BRCA samples

To examine the potential mechanism of *ZNF831* down-regulation in BRCA, we evaluated epigenetic and genetic alteration through SMART and the cBioPortal database. The results revealed 3 CG sites (cg25325636, cg16473762, cg09642670; Fig. S2A–C) were hypermethylated in the promoter region across many human cancers. The aggregation of cg25325636, cg16473762, and cg09642670 site methylation values showed the same trend (Fig. S2D). Among them, the methylation level of *ZNF831* was all higher in BRCA tissue than normal ($P < 0.05$) (Fig. 2A), ($P < 0.001$) (Fig. 2B), ($P < 0.0001$) (Fig. 2C). The aggregation of cg25325636, cg16473762, and cg09642670 site methylation values showed the same trend in BRCA tissue than normal ($P < 0.0001$) (Fig. 2D). In addition, we found that *ZNF831* expression levels were increased after demethylation treatment (decitabine) in MDA-MB-231 ($P < 0.001$) and MCF-7 ($P < 0.05$) BRCA cells (Fig. 2E), proving methylation involved in the down-regulation of *ZNF831*. Conversely, *ZNF831* somatic mutation rates (Fig. 2F) and DNA copy-number alterations (sCNA) (Fig. 2G) were low in most cancer types. As for BRCA, alteration frequency was low in all four data subsets (Fig. 2H–K). It suggested that promoter methylation, but not mutation or sCNA, was associated with *ZNF831* down-regulation in BRCA.

ZNF831 inhibits proliferation and promotes apoptosis of BRCA *in vitro*

To investigate the role of *ZNF831* in BRCA oncogenesis, we analyzed the expression of *ZNF831* in four BRCA cell lines (MDA-MB-231, MCF-7, BT474, HCC38) and one normal breast tissue cell line (MCF-10A). We found that *ZNF831* expression was relatively higher in HCC38 cells and relatively lower in MDA-MB-231, MCF-7, and BT474 cells than that in MCF-10A (Fig. 3A). So, we expressed ectopic *ZNF831* by Pcdna3.1-3xFLAG vector in MDA-MB-231, MCF-7, and BT474 (Fig. 3B) and knocked it down in HCC38 (Fig. 3C). The result from proliferation assay showed that over-expression of *ZNF831* inhibited cell proliferation (Fig. 3D–F) and knockdown of *ZNF831* could promote the proliferation (Fig. 3G). Over-expression of *ZNF831* resulted in a significant reduction of colony formation (Fig. 3H, I). In contrast, the knockdown of endogenous *ZNF831* in HCC38 increased cell viability (Fig. 3J, K). Besides, we found that *ZNF831* triggered BRCA cell apoptosis (Fig. 3L–N) and representative images were presented in Figure S3A–C. The rate of cell apoptosis was decreased with *ZNF831* knockdown (Fig. 2O) and representative images were presented in Figure S3D. Collectively, these data indicated that *ZNF831* was a suppressor in BRCA.

Genome-wide screening of potential target and pathway of promoting apoptosis for *ZNF831* by bioinformatics modeling

To explore the molecular mechanism underlying tumor suppressive effects of *ZNF831* in BRCA, we first analyzed the correlated genes through the LinkedOmics database and found there were 12,693 genes ($P < 0.05$) correlated with *ZNF831* in the "LinkFinder" part, 8108 genes were positively associated and 4585 genes were negatively associated (Fig. S4A). The top 50 significant genes positively and negatively correlated with *ZNF831* were shown in the heat map (Fig. 4A, B). A total description of the associated genes was detailed in Table S4. In the "LinkInterpreter" module, significant Gene Ontology (GO) annotations showed that all these associated genes were negatively associated with transcription by RNA polymerase I (FDR > 0.05), DNA-templated transcription (elongation) (FDR >0.05), and DNA-templated transcription (termination) (FDR > 0.05) in biological process (Fig. 4C). As for Kyoto Encyclopaedia of Genes and Genomes (KEGG) pathways, associated genes were negatively associated with RNA polymerase-related pathway (FDR < 0.05) and basal transcription factors (FDR >0.05) (Fig. 4D). To further forecast the potential tumor-suppressive mechanism of *ZNF831*, we carried out a Gene Set Enrichment Analysis (GSEA) of *ZNF831* with KEGG gene sets in TCGA-BRCA cohort. With 1215 samples and 20,530 genes in the analysis, we adopted the median cut-off value of ZNF831 to divide the 1215 samples into phenotype high group and low group. RNA polymerase-associated KEGG pathway was enriched in the low group (Fig. 4E); while *JAK/STAT* signal pathway and apoptosis-associated pathways were enriched in the high group (Fig. 4F). These results reminded us that *ZNF831* may play a tumor suppressor and participate in transcriptional regulation process and apoptotic pathways, including *JAK/STAT* pathway. Then, we identified differentially expressed genes between the vector group and the *ZNF831* ectopic over-expressed group in the MDA-MB-

Genetic alteration frequency of *ZNF831* was observed from the cBioPortal online tool in four BRCA studies of TCGA ((H) TCGA, Cell 2015; (I) TCGA, Firehouse legacy; (J) TCGA, Nature 2012; (K) TCGA, Pan-cancer atlas) and genomic profiles were limited in mutations and putative copy-number alteration from GISTIC. BRCA, breast carcinoma or breast cancer; qRT-PCR: real-time quantitative polymerase chain reaction; sCNA, somatic DNA copy-number alterations. $^{*}P < 0.05$, $^{***}P < 0.001$, $^{****}P < 0.0001$.

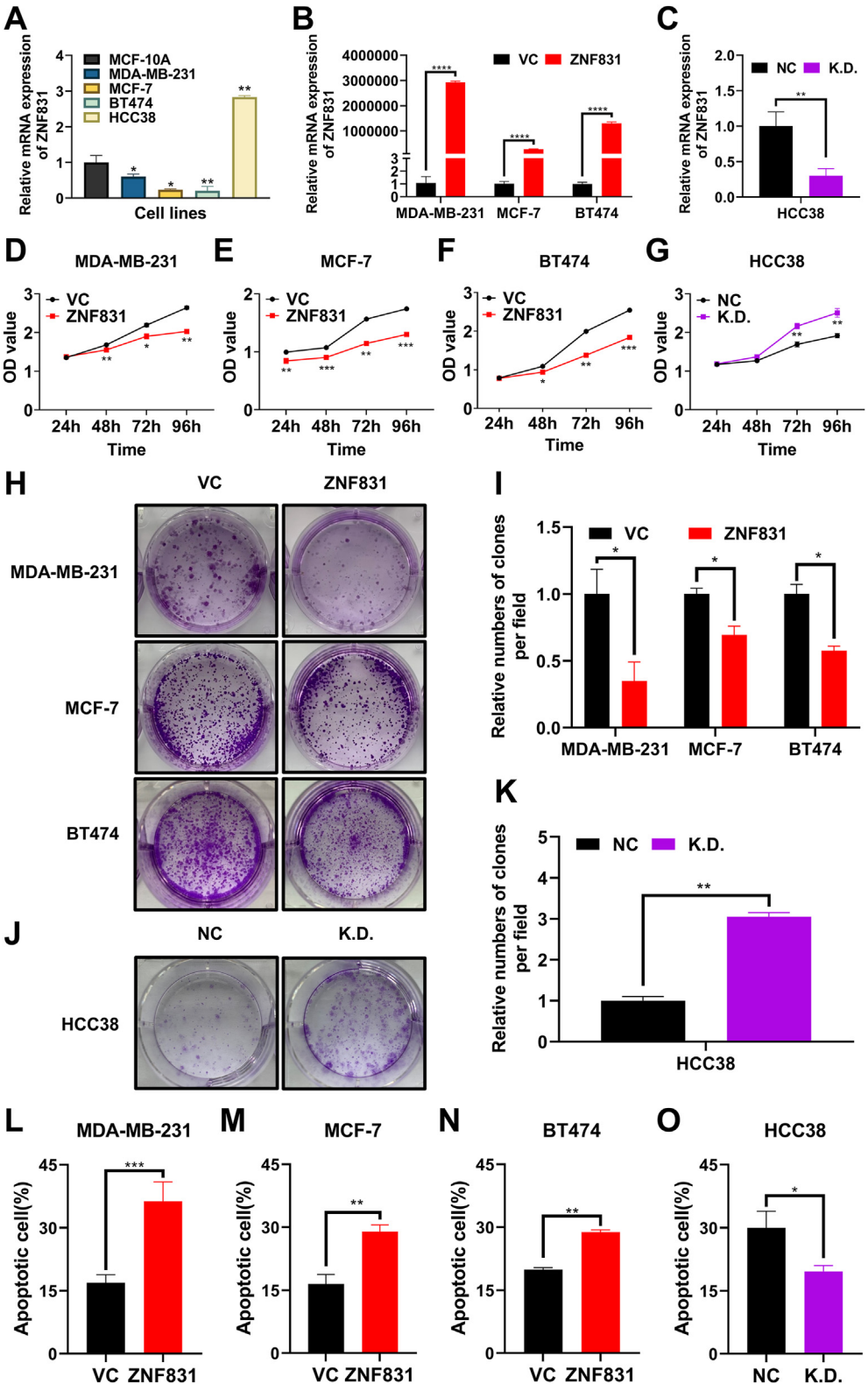

Figure 3 *ZNF831* inhibits proliferation and promotes apoptosis of BRCA *in vitro*. **(A)** *ZNF831* expressed relatively high in the HCC38 cell line and relatively low in MDA-MB-231, MCF-7, and BT474 cell lines compared to MCF-10A. **(B)** Ectopic *ZNF831* expression in MDA-MB-231, MCF-7, and BT474 cell lines were measured by qRT-PCR. **(C)** Expression of *ZNF831* knockdown in the HCC38 cell line was measured by qRT-PCR. **(D—F)** Proliferation assays were used to determine the proliferation effect of *ZNF831* over-expression on (D) MDA-MB-231, (E) MCF-7, and (F) BT474 cells. **(G)** A proliferation assay was used to determine the proliferation effect of *ZNF831* knockdown on HCC38 cells. **(H, I)** Colony formation assays were used to determine the proliferation effect of *ZNF831* over-expression on MDA-MB-231, MCF-7, and BT474 cells. (H) Representative images and (I) quantification plots were presented. **(J, K)** A

231 cells by RNA sequencing. A total of 778 differentially expressed genes (441 up-regulated and 337 down-regulated mRNAs, $P < 0.05$) were obtained (Fig. 4G) and these genes were detailed in Table S5. Regulation of transcription (DNA-templated) ($P < 0.001$), negative regulation of transcription (DNA-templated) ($P < 0.05$), transcription (DNA-templated) ($P < 0.001$), and RNA splicing ($P < 0.01$) associated biological processes were obtained by GO enrichment in up-regulated genes (Fig. 4H). Meanwhile, activation of Janus kinase activity ($P < 0.05$) associated biological process was obtained by GO enrichment in down-regulated genes (Fig. 4I). Signal transduction and cancer-related pathways were enriched in a considerably high percentage (Fig. S4B). Considering that *JAK/STAT* pathway and Janus kinase activity-associated biological process were enriched and both of them were apoptosis-related, we aimed at figuring out the key role in *ZNF831*-associated *JAK/STAT* family members.

ZNF831 induces cell apoptosis through direct binding to the specific site of the *STAT3* promoter region and transcriptionally suppresses *STAT3* expression in BRCA cell lines

To define the underlying molecular mechanism by which *ZNF831* induces apoptosis promotion, we focused on apoptosis-related star molecules of the *JAK/STAT* pathway. Firstly, we evaluated the mRNA level of *STAT3* and protein expression of STAT3 and P-STAT3 in BRCA cell lines which differentially expressed *ZNF831*, on account of its vital status in the *JAK/STAT* pathway. Transcriptionally, *STAT3* was down-regulated with the ectopic over-expression of *ZNF831* in MDA-MB-231 and BT474 (Fig. 5A, B), which was consistent with protein change (Fig. 5D); Whereas, whereas the knockdown of *ZNF831* increased *STAT3* expression both in mRNA (Fig. 5C) and protein level (Fig. 5D) in HCC38. The phosphorylated form of STAT3 was evaluated and the variation of P-STAT3 was consistent with the STAT3 (Fig. 5D). To further explore the change of the *STAT3/Bcl2* apoptotic pathway, we evaluated the protein level of Bcl2 and Bax. After the over-expression of *ZNF831*, Bcl2 was down-regulated when Bax was not changed in MDA-MB-231 and BT474 (Fig. 5D); whereas, knockdown of ZNF831 increased Bcl2 but no change in Bax in HCC38 (Fig. 5D). Coincidently, the variation of Bcl2 was consistent with the upstream STAT3 change. Then, we applied ectopic *STAT3* over-expression to explore whether amelioration of STAT3 rescued the apoptosis-promoting function induced by enhanced expression of *ZNF831* in breast cancer. Restored expression of STAT3 reversed the promotion of apoptosis in MDA-MB-231 and BT474 cell lines (Fig. 5E, F) and representative images were presented in Figure S5A and B. STAT3 and P-STAT3 were successfully ameliorated in *ZNF831* and *STAT3* co-expressed MDA-MB-231 and BT474 cell lines (Fig. 5G). Moreover, the attenuation of Bcl2 was offset by the restoration (Fig. 5G). One important question that still needed to be addressed was whether ZNF831 directly targeted the *STAT3* promoter in BRCA cells. To answer this question, we performed ChIP-qPCR assays using anti-FLAG antibodies with five promoter primers in different sequence positions according to the upstream 2000 bp region of NC_000017.11 (42313324..42388502, complement) (NCBI *STAT3* sequence) of *STAT3* (Fig. 5H). Only one of these primers was enriched in *ZNF831* ChIP-qPCR assay and the relative amount of *STAT3* promoter was higher in *ZNF831*-overexpressing cells, suggesting the occupancy of ZNF831 on the precise region of *STAT3* promoter (Fig. 5I). Furthermore, to confirm the suppression of *STAT3* expression in BRCA cells was directly mediated by ZNF831, we constructed *STAT3* promoters into the PGL3 plasmid and detected luciferase activity. We found that ectopic over-expression of *ZNF831* decreased the activity of the *STAT3* promoter by luciferase assay (Fig. 5J, K). These results were consistent with the negative correlation of *ZNF831* and *STAT3* expression in transcription and protein levels. All these data provided evidence that ZNF831 directly bound to and suppressed the endogenous *STAT3* promoter.

ZNF831 enhances chemosensitivity to capecitabine and gemcitabine in BRCA cell lines

To assess the potential relationship between *ZNF831* and chemoresistance in BRCA cells, we next investigated whether *ZNF831* affects BRCA cells' response to chemotherapy drugs. We found that ectopic over-expression of *ZNF831* promoted MDA-MB-231, MCF-7, and BT474 more sensitive to capecitabine (Fig. 6A—C) and gemcitabine (Fig. 6E—G). Knockdown of *ZNF831* reduced the sensitivity of HCC38 to capecitabine (Fig. 6D) and gemcitabine (Fig. 6H). In the comparison between capecitabine and gemcitabine, MDA-MB-231, MCF-7, and BT474 showed more sensitivity to gemcitabine after the augmented expression levels of *ZNF831*. Precisely, the degree of variation of chemosensitivity to capecitabine in MDA-MB-231 (Fig. 6A) is greater than MCF-7 (Fig. 6B) and BT474 (Fig. 6C) after the enhanced expression of *ZNF831*. Analogously, the degree of variation of chemosensitivity to gemcitabine in BT474 (Fig. 6G) is greater than MDA-MB-231 (Fig. 6E) and MCF-7 (Fig. 6F) after the enhanced expression of *ZNF831*. Taken together, these data further supported a critical function of *ZNF831* in regulating the response of BRCA cells to capecitabine and gemcitabine chemotherapy and suggested that a therapeutic approach targeting *ZNF831* may offer a route to overcome capecitabine and gemcitabine resistance.

colony formation assay was used to determine the proliferation effect of *ZNF831* knockdown on HCC38 cells. (J) Representative images and (K) quantification plots were presented. **(L—N)** Flow cytometric analysis of cell apoptosis of *ZNF831* over-expression on (L) MDA-MB-231, (M) MCF-7, and (N) BT474 cells with Annexin V-APC/7-AAD double staining. Statistical plots were presented. **(O)** Flow cytometric analysis of cell apoptosis of *ZNF831* knockdown on HCC38 with Annexin V-APC/7-AAD double staining. Statistical plots were presented. BRCA, breast carcinoma or breast cancer; qRT-PCR: real-time quantitative polymerase chain reaction; VC: vector control; NC: negative control; K.D.: knockdown. $^{*}P < 0.05$, $^{**}P < 0.01$, $^{***}P < 0.001$, $^{****}P < 0.0001$.

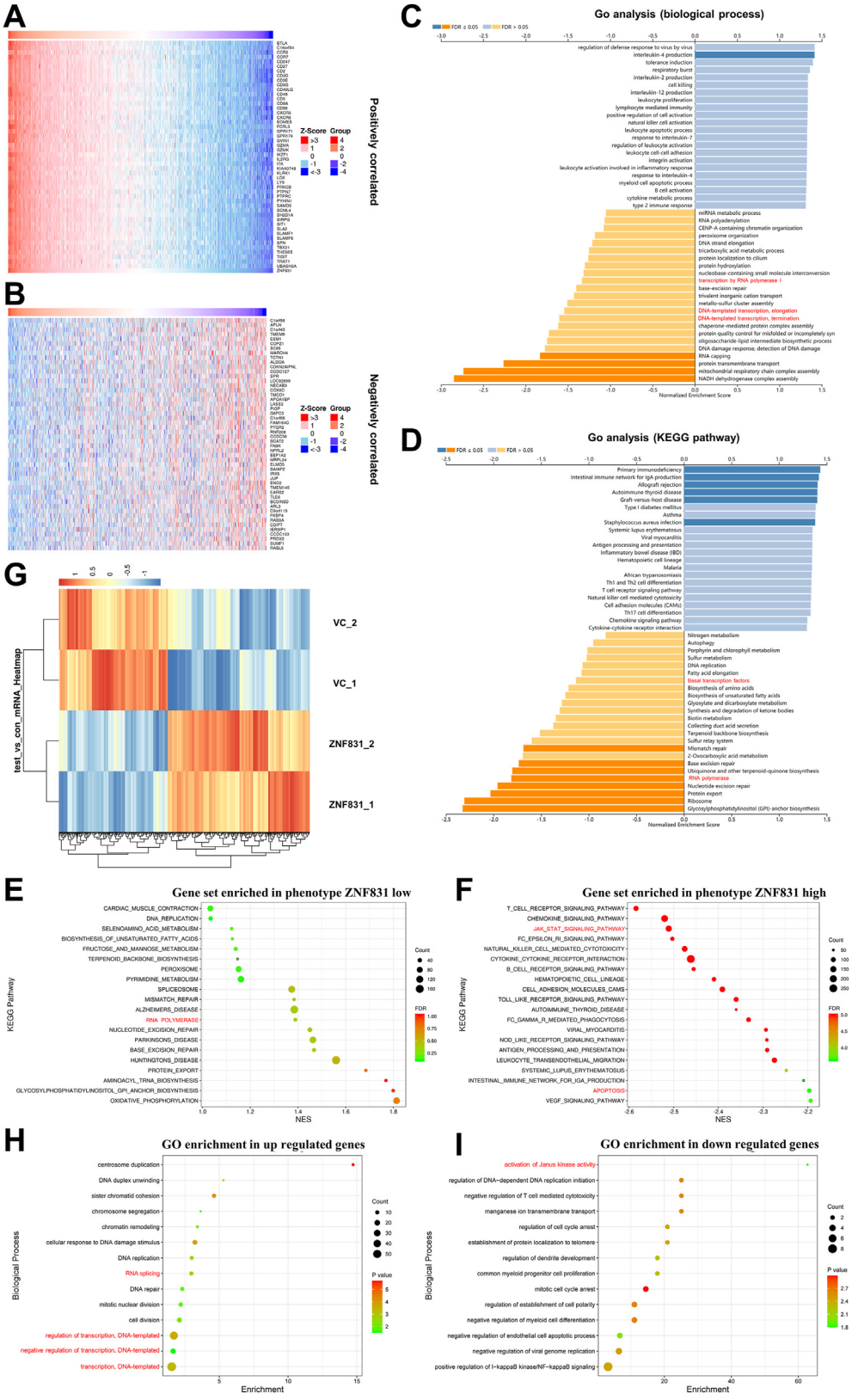

Figure 4 Genome-wide screening of potential target and pathway of promoting apoptosis for *ZNF831* by bioinformatics modeling. **(A, B)** Important positively (A) and negatively (B) correlated genes with *ZNF831* through the LinkedOmics database, TCGA_BRCA was selected as the cancer cohort and the platform of HiSeq RNA was chosen as the search and target dataset. **(C, D)** Bar charts of interesting (C) biological processes and (D) KEGG pathways of *ZNF831* associated genes with GO enrichment from LinkedOmics. **(E, F)** Bubble charts of interesting KEGG pathways enriched by the GSEA app in phenotype (E) *ZNF831*-low and (F) *ZNF831*-high group

ZNF831 suppresses BRCA cell proliferation *in vivo*

To verify the tumor-suppressive effect of *ZNF831 in vivo*, stable transfected BT474 cells with *ZNF831* over-expression were subcutaneously injected into BALB/c nude mice. The attenuation of growth rate and tumor weight was observed in BT474-*ZNF831* cells compared with the vector group (Fig. 7A–D). The volume of tumor mass formed in the over-expressed *ZNF831* group was significantly lower than that of the control group (Fig. 7A, B) and the growth rate of the overexpressed *ZNF831* group was significantly lower (Fig. 7C). The weight of the tumor in overexpressed *ZNF831* group was significantly lower (Fig. 7D). IHC staining results verified the ectopic expression of *ZNF831* and showed that over-expression of *ZNF831* significantly augmented the levels of TUNEL and mitigated *Ki-67* expression (Fig. 7E–H). Altogether, these results indicated that *ZNF831* suppressed tumor growth *in vivo*, which is consistent with our results *in vitro*.

Discussion

ZNF831, a member of the zinc finger protein family, is a protein coding gene and located in chromosome 20. It has been reported that *ZNF831* was correlated with BRCA stem cell phenotype and relapse risk of patients.[30] Several studies have indicated that *ZNF831* was involved in immune regulation[30,31] and preeclampsia.[32] Notwithstanding, the role and mechanism of *ZNF831* in tumorigenesis remain unclear. In this study, we demonstrated that *ZNF831* was down-regulated due to promoter methylation and repressed the cell proliferation, and promoted apoptosis through transcriptional attenuation of *STAT3* expression in BRCA (Fig. 8). These findings not only significantly enriched our understanding of the tumor suppressor function of *ZNF831* in BRCA but also indicated a new therapeutic strategy for BRCA treatment for the first time.

In our study, the transcriptome data from the Timer database showed *ZNF831* was diminished in most cancer types, including BRCA. The expression difference was confirmed by Oncomine and TCGA BRCA database, which suggested *ZNF831* might play a vital role in breast carcinogenesis. It has been confirmed many ZNFs were down-regulated or disabled in BRCA as tumor suppressors. The GATA-type zinc finger transcription factor *TRPS1* was a context-dependent tumor suppressor and loss of function promoted oncogenesis in lobular breast carcinoma.[33] Restraint of *UBR7* enhanced the invasiveness, induced epithelial-to-mesenchymal transition, and promoted metastasis in BRCA.[34]

As one of the major ways of gene expression regulation, epigenetic modification contained many methods including DNA methylation, histone modification, chromatin remodeling, and RNA regulation.[35] DNA methylation down-regulated ZNFs expression was a common way in cancer. *ZNF377* was down-regulated by DNA methylation and suppressed tumor growth by altering cellular metabolism and inducing apoptosis and pyroptosis.[36] *ZNF471* was an important tumor suppressor and was frequently silenced by promoter CpG methylation in esophageal cancer.[37] We figured out promoter methylation but not mutation or copy number variation as a promising reason and a potential researching candidate for restraint of *ZNF831* in BRCA. Of course, many new-found ways regulated the expression of ZNFs, like lncRNA and miRNA modulation. For example, *lnc01060* directly interacted with the transcription factor myeloid zinc finger 1 and enhanced its stability to regulate the progression of glioma.[38] *MicroRNA-181a* modulated gene expression of ZNFs by directly targeting their coding regions.[39] Post-transcriptional regulation of gene expression is a hotspot of scientific research in cancer. As N6-methyladenosine (m6A) RNA methylation, *YTHDF3* enhanced the translation of m6A-enriched transcripts to promote BRCA brain metastasis.[40] So, RNA modification and post-transcriptional regulation of *ZNF831* would be the potential target for our future study.

Functional studies revealed that ectopic over-expression of *ZNF831* decreased the proliferation and colony formation and promoted cell apoptosis in BRCA. Many cancer suppressors played roles in antitumor progression in similar ways. Endothelial *miR-30c* suppressed tumor growth by promoting fibrin degradation and inhibiting blood vessel formation in the tumor microenvironment.[41] *ALOX12*-mediated ferroptosis pathway was critical for *p53*-dependent tumor suppression.[42] In this way, combining the low expression of *ZNF831* in BRCA and anti-tumor functions, *ZNF831* is strong enough to be a suppressor in BRCA. But the potential roles of *ZNF831* in other aspects are to be explored. Considering *ZNF831* was an immune regulator and $CD8^+$ T cells regulate tumor ferroptosis during cancer immunotherapy, *ZNF831* might play a role in the ferroptosis of BRCA.[43] Or like other reported ZNFs, *E4F1* promoted DNA double-strand break repair.[44] *ZNF322A* promoted stem cell-like properties in lung cancer by acting as a transcription suppressor of *c-Myc*.[45] *ZDHHC1* exerted significant pyroptosis-promoting effects through metabolic regulation.[36] Autophagy, senescence, oxidative stress, and tumor micro-environment were also influenced by ZNFs.[28,46–48]

To figure out the details of the tumor-suppressive mechanism of *ZNF831* in BRCA, we explored the *ZNF831*-related KEGG pathways and biological processes through public databases and transcriptome sequencing in the BRCA cell line. Apoptosis, *JAK/STAT* pathway, and transcriptional regulation were enriched in many items. Therefore, we supposed that *ZNF831* regulated BRCA cell apoptosis through *JAK/STAT* pathway. *STAT3* was a key member of the

through TCGA genomic matrix. **(G)** Transcriptome sequence difference in ectopic *ZNF831* expression group and control group of MDA-MB-231 cells. **(H, I)** Bubble charts of interesting biological processes enriched in (H) up-regulated and (I) down-regulated gene sets from transcriptome sequence in MDA-MB-231 cells. BRCA, breast carcinoma or breast cancer; KEGG: Kyoto Encyclopedia of Genes and Genomes; GO: gene ontology; GSEA: gene set enrichment analysis; TCGA: the Cancer Genome Atlas.

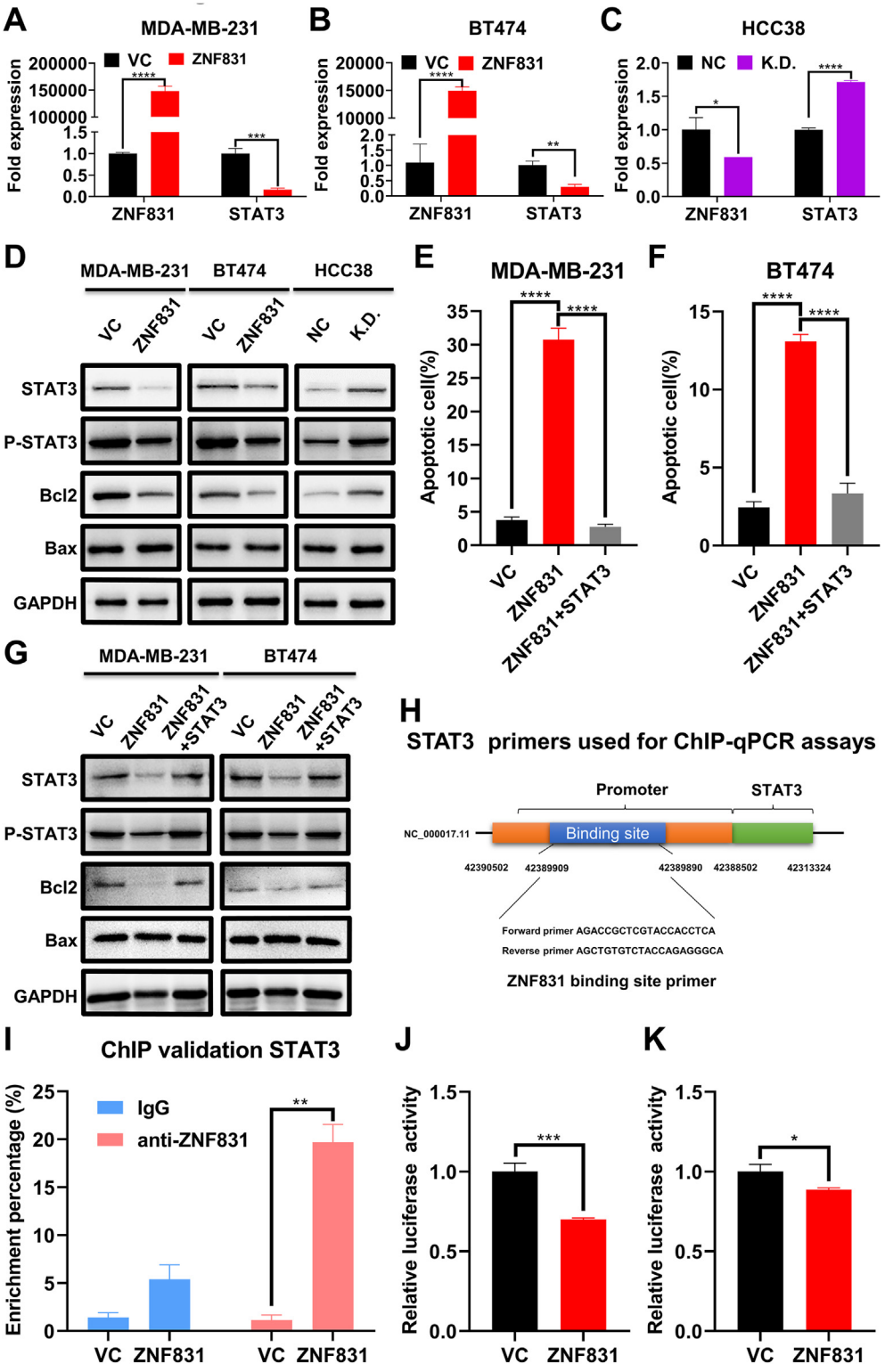

Figure 5 ZNF831 induces cell apoptosis through directly binding to the specific site of the *STAT3* promoter region and transcriptionally suppresses *STAT3* expression in BRCA cell lines. **(A, B)** Evaluation of the transcriptional level of *STAT3* in (A) MDA-MB-231 and (B) BT474 cells which were characterized by ectopic *ZNF831* expression. **(C)** Evaluation of the transcriptional level of *STAT3* in HCC38 cells which were characterized by *ZNF831* knockdown. **(D)** Evaluation of protein level of STAT3, P-STAT3, Bcl2, and Bax in MDA-MB-231 and BT474 cell lines which were characterized by ectopic *ZNF831* expression, and in HCC38 cells which were characterized by *ZNF831* knockdown. GAPDH was used as a loading control. **(E, F)** Flow cytometric analysis of cell apoptosis of ectopic *ZNF831* and *STAT3* co-overexpression on (E) MDA-MB-231 and (F) BT474 cell lines with Annexin V-APC/7-AAD double staining.

STAT family and a cytoplasmic transcription factor that regulates cell proliferation, stem cell-like characteristics, differentiation, apoptosis, angiogenesis, inflammation, and immune responses.[49–54] It was a point of convergence for numerous oncogenic signaling pathways and played an important role in the transcription of downstream target genes during oncogenesis.[55] *STAT3* mitigated BRCA cell apoptosis through transcriptional activation of *Bcl2* expression.[56] Importantly, *STAT3* was central in regulating the anti-tumor immune response and played a role in inhibiting the expression of crucial immune activation regulators and promoting the production of immunosuppressive factors.[57] As mentioned before (Fig. 1, 3), *ZNF831* was diminished in breast cancer, and enhanced *ZNF831* attenuated cell proliferation and colony formation abilities, and augmented apoptosis of cells. Through RNA sequencing and gene expression level detection, we speculated that *STAT3* is a potential target after the augmentation of *ZNF831*. So, we aimed at *STAT3* to explore the relationship between *ZNF831* with its classic *STAT3*/*Bcl2* apoptotic pathway.

Mechanistically, we figured out that *ZNF831* transcriptionally inhibited *STAT3* expression by binding to the specific site of the *STAT3* promoter region to regulate the oncogenesis of BRCA. Moreover, it has been reported that SD-36, a small-molecule degrader, induced the degradation of *STAT3* protein and achieved complete tumor regression.[58] Resistance to durvalumab and durvalumab plus tremelimumab induced by functional *STK11* mutations in non-small-cell lung cancer patients could be reversed by *STAT3* knockdown.[59] Therefore, we could see the importance of the regulation between *ZNF831* and *STAT3* and there were many unknown functions induced by *ZNF831*/*STAT3* pathway to be explored.

Except for transcriptional regulation, there were many other possible regulation mechanisms to influence *STAT3* like methylation, acetylation, ubiquitination, and palmitoylation.[53] Sulfhydration of *SIRT1* suppressed phosphorylation and acetylation of *STAT3*.[60] Protein–protein interaction to induce phosphorylation or acetylation was an important way to regulate protein activity. Especially, *STAT3* is activated by the phosphorylation of residues Y705 and S727 to mediate the transcription of downstream genes.[61] Palmitoylation was another way to influence *STAT3* by ZNFs, as *ZDHHC19* promoted *STAT3* activation through S-palmitoylation.[62] Considering ZNFs were associated with the production of non-coding RNA,[63] *FLANC*, long non-coding RNA in colorectal cancer, up-regulated and prolonged the half-life of phosphorylated *STAT3*.[64] Furthermore, according to the self-regulation of *STAT3* through transcriptional regulation by binding to the promoter region of *STAT3* gene, we raise a presumption that *ZNF831* interacts with *STAT3* to form a transcription–initiation complex to inhibit transcription of *STAT3*.[65] Of course, the protein–protein interaction analysis and co-immunoprecipitation assay are needed to support the corresponding presumption.

Chemotherapeutic agents, such as capecitabine and gemcitabine, hold the backbone of treatment for many solid tumors including BRCA and hepatocellular carcinoma, but the development of resistance is a major stumbling block of treatment.[66] In clinics, BRCA patients are frequently resistant to chemotherapy, especially advanced ones. Figuring out the mechanism of chemoresistance and identifying the biomarker of resistance will be the top priority of modern medicine for overcoming this limitation and for the development of effective therapy. Gemcitabine and capecitabine were the cornerstone of cancer therapy for the improvement of overall survival.[67,68] Importantly, we found out that the chemical sensitivity of capecitabine and gemcitabine could be ameliorated by enhanced expression of *ZNF831*. This provided us with a new insight into chemical therapy in BRCA patients. But the mechanism of the chemical sensitivity amelioration is yet to be explored. It has been reported that *JAK*/*STAT3* pathway and its downstream fatty acid β-oxidation are critical for BRCA stem cell chemoresistance.[69] Circadian melatonin disruption mediated *STAT3*-driven paclitaxel resistance in breast cancer.[70] So, there would be a potential mechanism of chemoresistance that stayed behind the *ZNF831*/*STAT3* pathway. What's more, the degree of variation of chemosensitivity to capecitabine in MDA-MB-231 and the degree of variation of chemosensitivity to gemcitabine in BT474 were respectively greater in three BRCA cell lines. It showed us that *ZNF831*-induced chemosensitivity enhancement was tumor type-specific and the mechanisms behind played in diversity.

In summary, we first showed that *ZNF831* was a BRCA suppressor that prevented BRCA cell proliferation via transcriptionally diminishing the expression of *STAT3* to promote cell apoptosis. The multitude of the biological function of *ZNF831* is beyond what we have studied. Further studies are warranted to investigate the scope of mechanistic insights into the role of *ZNF831* in other malignancies. Precise *ZNF831*-*STAT3* promoter binding site sequence and mutation verification test could provide valuable information for target therapy of the *ZNF831*/*STAT3* pathway. The mechanism of ameliorated chemosensitivity in an enhanced level of *ZNF831* expression in BRCA cells supports the clinical development of novel therapies targeting the *ZNF831* for the treatment of human BRCA. Notably, data from public databases and transcriptome sequencing provided us with a new clue that *ZNF831* is probably a potentially key role in tumor immunity. So, research about BRCA immunity has been placed on the agenda.

Statistical plots were presented. **(G)** Evaluation of protein level of STAT3, P-STAT3, Bcl2, and Bax in MDA-MB-231 and BT474 cells which were characterized by ectopic *ZNF831* and *STAT3* co-overexpression. **(H)** The schematic plot showed the location of the *STAT3* primer used and detected in ChIP-qPCR assays. **(I)** Detection enrichment percentages of the specific promoter region of *STAT3* by qPCR followed by ChIP with anti-FLAG antibody. **(J, K)** The effect of ectopic *ZNF831* expression on the transcription of *STAT3* as determined by luciferase reporter activity assays. GAPDH was used as a loading control. VC: vector control; NC: negative control; K.D.: knock down; ChIP: chromatin immunoprecipitation. $^{*}P < 0.05$, $^{**}P < 0.01$, $^{***}P < 0.001$, $^{****}P < 0.0001$.

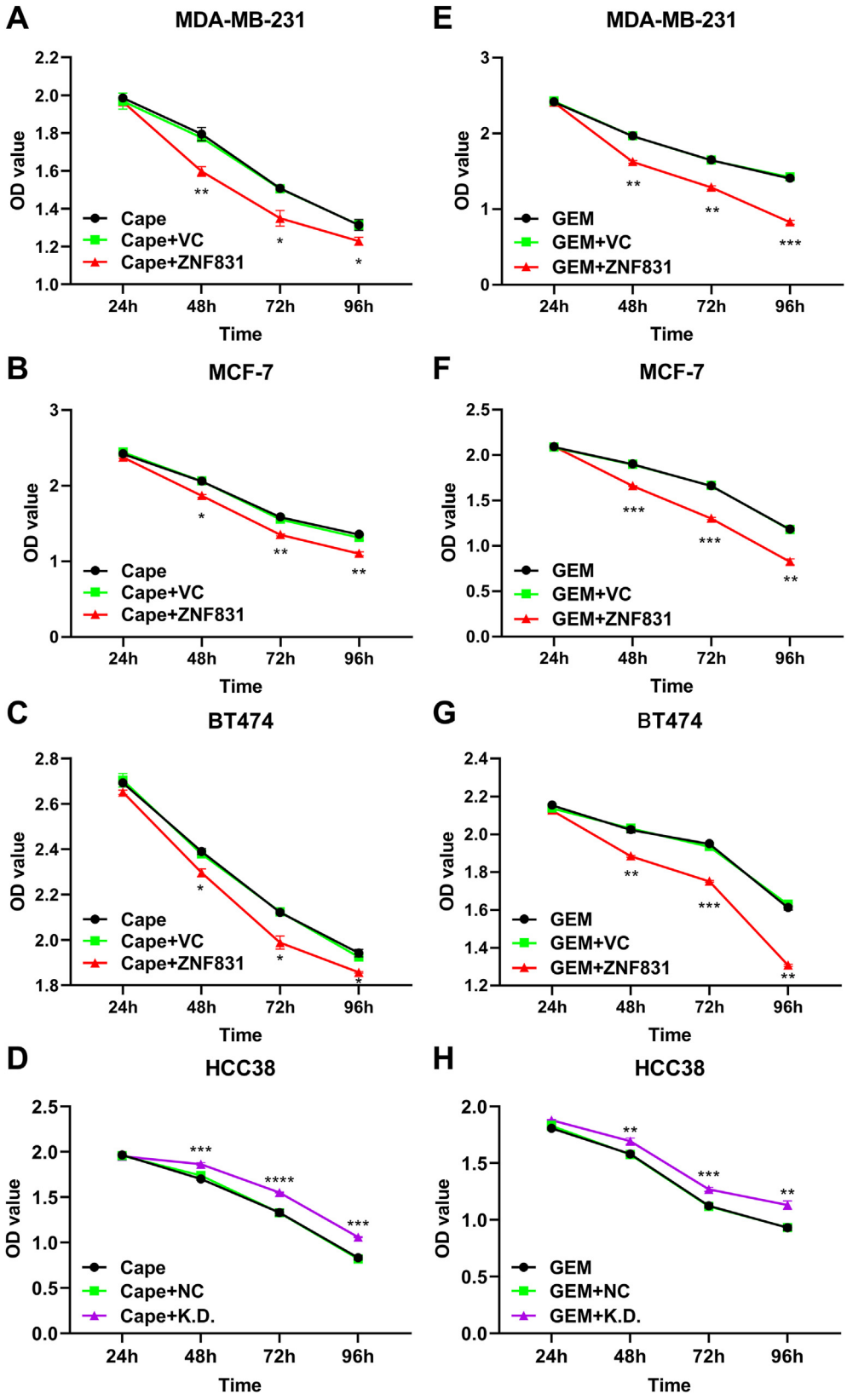

Figure 6 *ZNF831* enhances chemosensitivity to capecitabine and gemcitabine in BRCA cell lines. **(A—C)** Proliferation assay was used to determine the chemosensitivity of capecitabine in (A) MDA-MB-231, (B) MCF-7, and (C) BT474 cells which were characterized by ectopic *ZNF831* expression, and in **(D)** HCC38 cells which were characterized by *ZNF831* knockdown. **(E—G)** Proliferation assay was used to determine the chemosensitivity of gemcitabine in (E) MDA-MB-231, (F) MCF-7, and (G) BT474 cells which were characterized by ectopic *ZNF831* expression, and in **(H)** HCC38 cells which were characterized by *ZNF831* knockdown. Cape: capecitabine; GEM: gemcitabine. $^{*}P < 0.05$, $^{**}P < 0.01$, $^{***}P < 0.001$, $^{****}P < 0.0001$.

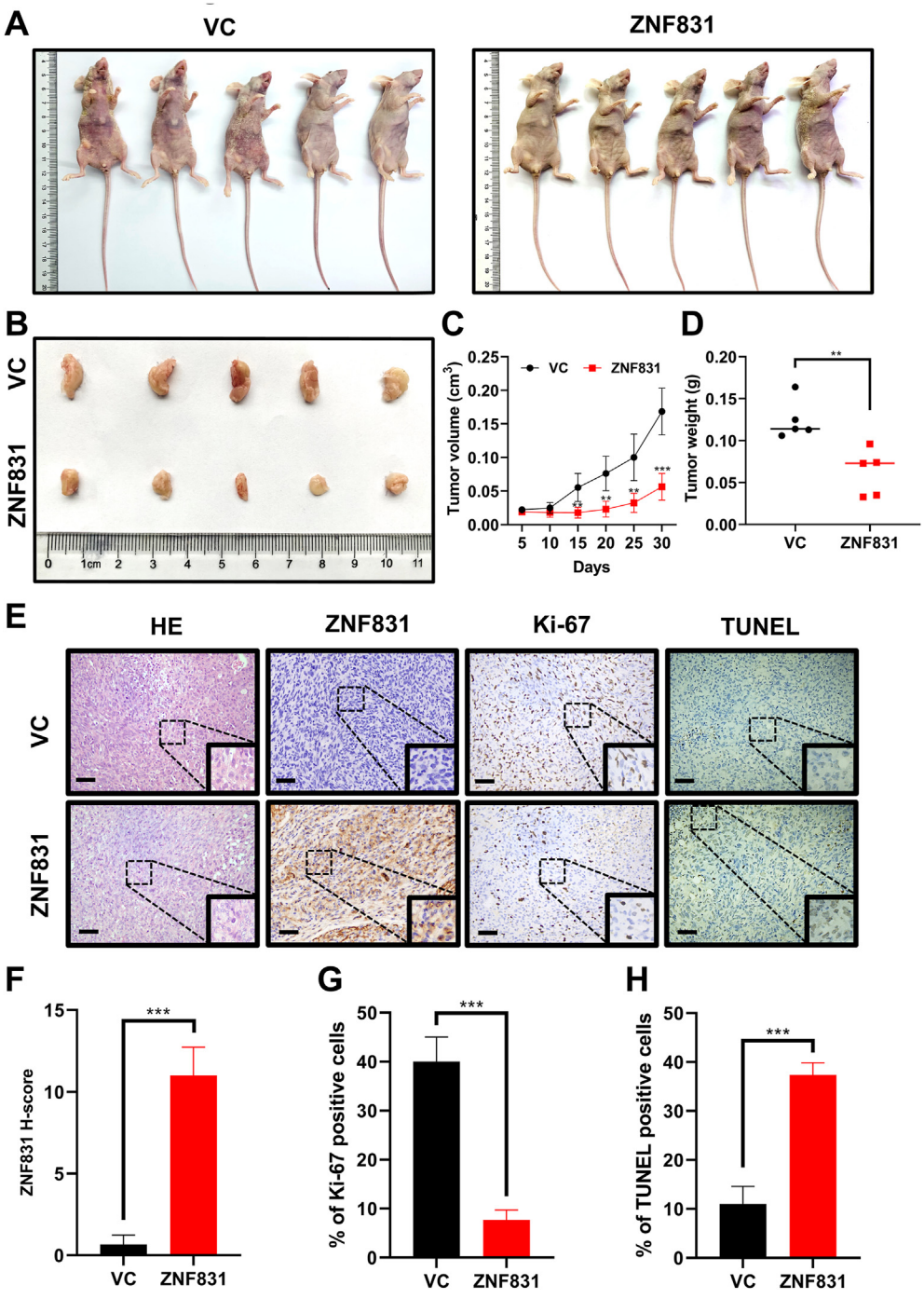

Figure 7 *ZNF831* suppresses BRCA cell proliferation *in vivo*. **(A, B)** The growth of tumors after subcutaneous injection of BRCA cells with *ZNF831* over-expression for 30 days in nude mice. (B) Representative images of tumor volumes from xenograft mice described above. **(C)** The growth of the tumor was observed every 5 days after subcutaneous injection of cells with or without over-expressing *ZNF831* gene. **(D)** After the tumor was removed, the weight of the tumor was measured. The data are shown as the means ± SD **(E)** Representative images of apoptosis detection in tumor sections from xenograft mice by TUNEL and immunohistochemistry staining for *ZNF831* expression and cell proliferation test (*Ki-67*) in tumor sections from xenograft mice were described above. **(F—H)** Quantification plots were presented. Scale bar = 100 μm. BRCA, breast cancer. $^{*}P < 0.05$, $^{**}P < 0.01$, $^{***}P < 0.001$.

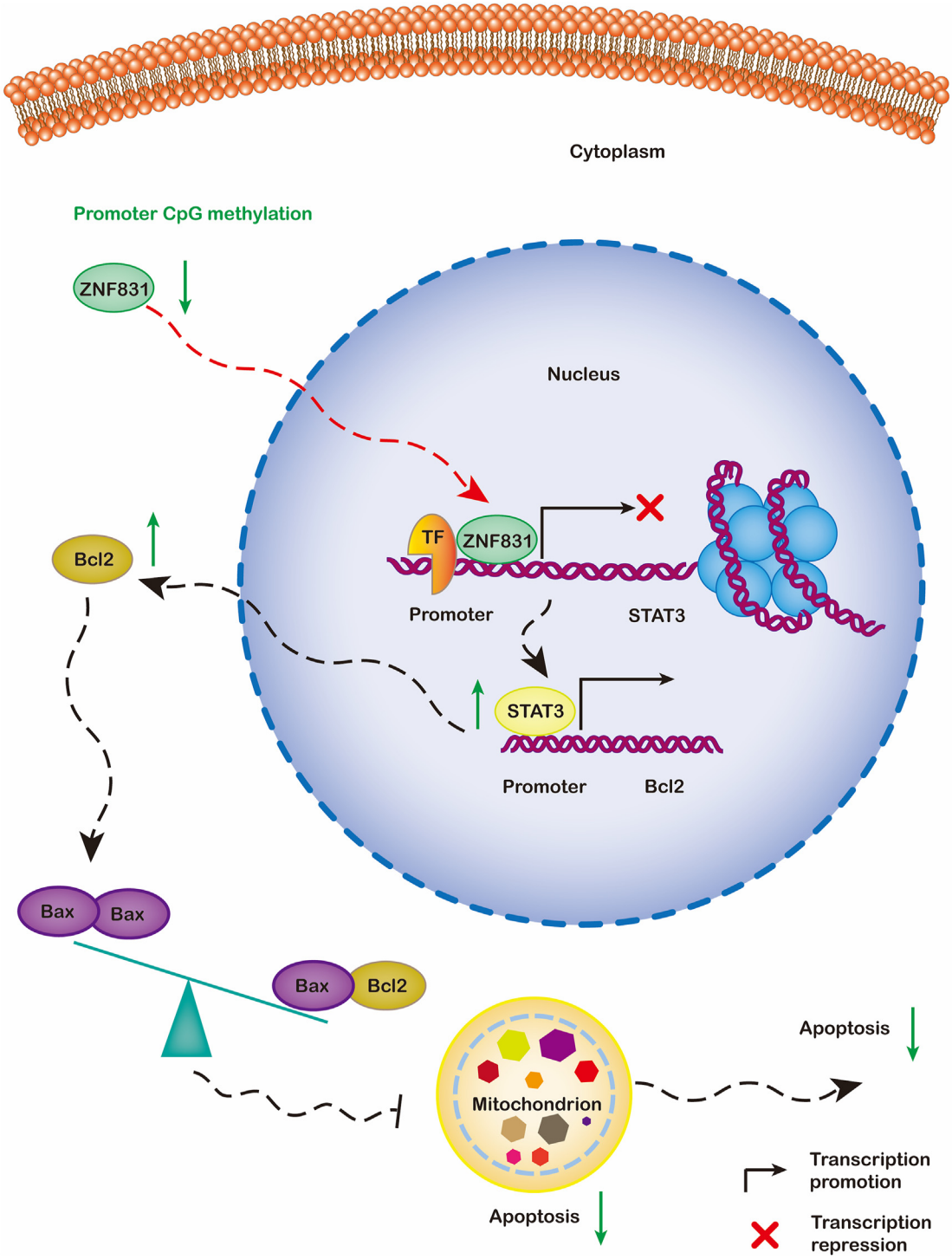

Figure 8 *ZNF831* induces BRCA cell apoptosis through *STAT3*/*Bcl2* axis. In mechanism, we proved that *ZNF831* could directly bind the promoter region of *STAT3* and transcriptionally down-regulated its expression to attenuate transcription of *Bcl2* which promoted the apoptosis of BRCA cells. The expression of *ZNF831* could be regulated by promoter CpG site methylation. BRCA, breast carcinoma or breast cancer; TF, transcriptional factor.

Ethical statement

The authors are accountable for all aspects of the work in ensuring that questions related to the accuracy or integrity of any part of the work are appropriately investigated and resolved. The study was approved by the Ethics Committee of Daping Hospital and the Laboratory Animal Welfare and Ethics Committee of the Third Military Medical University.

Author contributions

Concept and design: Jun Fan, Zhe Zhang, Wenbin Liu and Yan Xu; Administrative support: Wenbin Liu and Yan Xu; Provision of study materials or patients: Zhe Zhang, Dongjiao Chen, Hongqiang Chen, Wenbo Yuan, Jingzhi Li, Yong Zeng, Shimeng Zhou, Shu Zhang, Gang Zhang, Jiashen Xiong, Lu Zhou, and Jing Xu; Data acquisition, analysis, and statistical analysis: Jun Fan and Zhe Zhang; Experimental studies: Jun Fan; Manuscript preparation, editing, review, and literature search: all authors; Final approval of manuscript: all authors.

Conflict of interests

The authors have no conflict of interests to declare.

Funding

This work was supported by the National Natural Science Foundation of China (No. 81472482, 82173556), the Clinical Technology Innovation and Cultivation Project of the Army Medical University of China (No. CX2019LC120), and the National Key Clinical Specialty Military Construction Project (China, No. 425Z8).

Appendix A. Supplementary data

Supplementary data to this article can be found online at https://doi.org/10.1016/j.gendis.2022.11.023.

References

1. Britt KL, Cuzick J, Phillips KA. Key steps for effective breast cancer prevention. *Nat Rev Cancer*. 2020;20(8):417–436.
2. Sung H, Ferlay J, Siegel RL, et al. Global cancer statistics 2020: GLOBOCAN estimates of incidence and mortality worldwide for 36 cancers in 185 countries. *CA A Cancer J Clin*. 2021;71(3):209–249.
3. Nejman D, Livyatan I, Fuks G, et al. The human tumor microbiome is composed of tumor type-specific intracellular bacteria. *Science*. 2020;368(6494):973–980.
4. Wagner J, Rapsomaniki MA, Chevrier S, et al. A single-cell atlas of the tumor and immune ecosystem of human breast cancer. *Cell*. 2019;177(5):1330–1345. e18.
5. Coleman RE, Croucher PI, Padhani AR, et al. Bone metastases. *Nat Rev Dis Prim*. 2020;6:83.
6. Jin X, Demere Z, Nair K, et al. A metastasis map of human cancer cell lines. *Nature*. 2020;588(7837):331–336.
7. Xiao Y, Cong M, Li J, et al. Cathepsin C promotes breast cancer lung metastasis by modulating neutrophil infiltration and neutrophil extracellular trap formation. *Cancer Cell*. 2021;39(3):423–437.
8. Tsilimigras DI, Brodt P, Clavien PA, et al. Liver metastases. *Nat Rev Dis Prim*. 2021;7:27.
9. Turunen SP, von Nandelstadh P, Öhman T, et al. FGFR4 phosphorylates MST1 to confer breast cancer cells resistance to MST1/2-dependent apoptosis. *Cell Death Differ*. 2019;26(12):2577–2593.
10. Zeitler B, Froelich S, Marlen K, et al. Allele-selective transcriptional repression of mutant HTT for the treatment of Huntington's disease. *Nat Med*. 2019;25(7):1131–1142.
11. Wang Y, Yuan S, Jia X, et al. Mitochondria-localised ZNFX1 functions as a dsRNA sensor to initiate antiviral responses through MAVS. *Nat Cell Biol*. 2019;21(11):1346–1356.
12. Mirza AN, McKellar SA, Urman NM, et al. LAP2 proteins chaperone GLI1 movement between the *Lamina* and chromatin to regulate transcription. *Cell*. 2019;176(1–2):198–212.
13. Otten EG, Werner E, Crespillo-Casado A, et al. Ubiquitylation of lipopolysaccharide by RNF213 during bacterial infection. *Nature*. 2021;594(7861):111–116.
14. Lambert SA, Yang AWH, Sasse A, et al. Similarity regression predicts evolution of transcription factor sequence specificity. *Nat Genet*. 2019;51(6):981–989.
15. Beasley SA, Hristova VA, Shaw GS. Structure of the Parkin in-between-ring domain provides insights for E3-ligase dysfunction in autosomal recessive Parkinson's disease. *Proc Natl Acad Sci U S A*. 2007;104(9):3095–3100.
16. Deng Z, Lehmann KC, Li X, et al. Structural basis for the regulatory function of a complex zinc-binding domain in a replicative arterivirus helicase resembling a nonsense-mediated mRNA decay helicase. *Nucleic Acids Res*. 2014;42(5):3464–3477.
17. Fernández-Tornero C, Moreno-Morcillo M, Rashid UJ, et al. Crystal structure of the 14-subunit RNA polymerase I. *Nature*. 2013;502(7473):644–649.
18. Hagiwara D, Miura D, Shimizu K, et al. A novel Zn2-Cys6 transcription factor AtrR plays a key role in an azole resistance mechanism of *Aspergillus fumigatus* by Co-regulating cyp51A and cdr1B expressions. *PLoS Pathog*. 2017;13(1):e1006096.
19. He J, Ye J, Cai Y, et al. Structure of p300 bound to MEF_2 on DNA reveals a mechanism of enhanceosome assembly. *Nucleic Acids Res*. 2011;39(10):4464–4474.
20. Krishna SS, Majumdar I, Grishin NV. Structural classification of zinc fingers: survey and summary. *Nucleic Acids Res*. 2003;31(2):532–550.
21. Lin S, Wang X, Pan Y, et al. Transcription factor myeloid zinc-finger 1 suppresses human gastric carcinogenesis by interacting with metallothionein 2A. *Clin Cancer Res*. 2019;25(3):1050–1062.
22. Xiang T, Tang J, Li L, et al. Tumor suppressive BTB/POZ zinc-finger protein ZBTB28 inhibits oncogenic BCL6/ZBTB27 signaling to maintain p53 transcription in multiple carcinogenesis. *Theranostics*. 2019;9(26):8182–8195.
23. Liu M, Zhang Y, Yang J, et al. ZIP4 increases expression of transcription factor ZEB1 to promote integrin $\alpha 3\beta 1$ signaling and inhibit expression of the gemcitabine transporter ENT1 in pancreatic cancer cells. *Gastroenterology*. 2020;158(3):679–692.
24. Zhang Y, Zou X, Qian W, et al. Enhanced PAPSS2/VCAN sulfation axis is essential for Snail-mediated breast cancer cell migration and metastasis. *Cell Death Differ*. 2019;26(3):565–579.
25. Schuster A, Klein E, Neirinckx V, et al. AN1-type zinc finger protein 3 (ZFAND3) is a transcriptional regulator that drives Glioblastoma invasion. *Nat Commun*. 2020;11:6366.
26. Zhang L, Li J, Xu H, et al. Myc-Miz1 signaling promotes self-renewal of leukemia stem cells by repressing Cebpα and Cebpδ. *Blood*. 2020;135(14):1133–1145.
27. Phan RT, Dalla-Favera R. The BCL6 proto-oncogene suppresses p53 expression in germinal-centre B cells. *Nature*. 2004;432(7017):635–639.

28. Hu H, Ji Q, Song M, et al. ZKSCAN$_3$ counteracts cellular senescence by stabilizing heterochromatin. *Nucleic Acids Res*. 2020;48(11):6001—6018.
29. Singh SR, Meyer-Jens M, Alizoti E, et al. A high-throughput screening identifies ZNF418 as a novel regulator of the ubiquitin-proteasome system and autophagy-lysosomal pathway. *Autophagy*. 2021;17(10):3124—3139.
30. da Silveira WA, Palma PVB, Sicchieri RD, et al. Transcription factor networks derived from breast cancer stem cells control the immune response in the basal subtype. *Sci Rep*. 2017;7:2851.
31. He Y, Jiang Z, Chen C, et al. Classification of triple-negative breast cancers based on Immunogenomic profiling. *J Exp Clin Cancer Res*. 2018;37:327.
32. Steinthorsdottir V, McGinnis R, Williams NO, et al. Genetic predisposition to hypertension is associated with preeclampsia in European and Central Asian women. *Nat Commun*. 2020;11(1):5976.
33. Cornelissen LM, Drenth AP, van der Burg E, et al. TRPS1 acts as a context-dependent regulator of mammary epithelial cell growth/differentiation and breast cancer development. *Genes Dev*. 2020;34(3—4):179—193.
34. Adhikary S, Chakravarti D, Terranova C, et al. Atypical plant homeodomain of UBR7 functions as an $H_2BK_{120}Ub$ ligase and breast tumor suppressor. *Nat Commun*. 2019;10(1):1398.
35. Zhang W, Qu J, Liu GH, et al. The ageing epigenome and its rejuvenation. *Nat Rev Mol Cell Biol*. 2020;21(3):137—150.
36. Le X, Mu J, Peng W, et al. DNA methylation downregulated ZDHHC1 suppresses tumor growth by altering cellular metabolism and inducing oxidative/ER stress-mediated apoptosis and pyroptosis. *Theranostics*. 2020;10(21):9495—9511.
37. Sun R, Xiang T, Tang J, et al. 19q13 KRAB zinc-finger protein ZNF471 activates MAPK10/JNK3 signaling but is frequently silenced by promoter CpG methylation in esophageal cancer. *Theranostics*. 2020;10(5):2243—2259.
38. Li J, Liao T, Liu H, et al. Hypoxic glioma stem cell-derived exosomes containing Linc01060 promote progression of glioma by regulating the MZF1/c-myc/HIF1α axis. *Cancer Res*. 2021;81(1):114—128.
39. Huang S, Wu S, Ding J, et al. MicroRNA-181a modulates gene expression of zinc finger family members by directly targeting their coding regions. *Nucleic Acids Res*. 2010;38(20):7211—7218.
40. Chang G, Shi L, Ye Y, et al. YTHDF$_3$ induces the translation of m^{6}A-enriched gene transcripts to promote breast cancer brain metastasis. *Cancer Cell*. 2020;38(6):857—871.
41. McCann JV, Xiao L, Kim DJ, et al. Endothelial miR-30c suppresses tumor growth via inhibition of TGF-β-induced Serpine1. *J Clin Invest*. 2019;129(4):1654—1670.
42. Chu B, Kon N, Chen D, et al. ALOX12 is required for p53-mediated tumour suppression through a distinct ferroptosis pathway. *Nat Cell Biol*. 2019;21(5):579—591.
43. Wang W, Green M, Choi JE, et al. CD8$^+$ T cells regulate tumour ferroptosis during cancer immunotherapy. *Nature*. 2019;569(7755):270—274.
44. Moison C, Chagraoui J, Caron MC, et al. Zinc finger protein E4F1 cooperates with PARP-1 and BRG1 to promote DNA double-strand break repair. *Proc Natl Acad Sci U S A*. 2021;118(11):e2019408118.
45. Jen J, Liu CY, Chen YT, et al. Oncogenic zinc finger protein ZNF$_3$22A promotes stem cell-like properties in lung cancer through transcriptional suppression of c-Myc expression. *Cell Death Differ*. 2019;26(7):1283—1298.
46. Zhu L, Ding R, Yan H, et al. ZHX2 drives cell growth and migration via activating MEK/ERK signal and induces Sunitinib resistance by regulating the autophagy in clear cell Renal Cell Carcinoma. *Cell Death Dis*. 2020;11(5):337.
47. de Barrios O, Sanchez-Moral L, Cortés M, et al. ZEB1 promotes inflammation and progression towards inflammation-driven carcinoma through repression of the DNA repair glycosylase MPG in epithelial cells. *Gut*. 2019;68(12):2129—2141.
48. Zhang W, Zhangyuan G, Wang F, et al. The zinc finger protein Miz1 suppresses liver tumorigenesis by restricting hepatocyte-driven macrophage activation and inflammation. *Immunity*. 2021;54(6):1168—1185.
49. Huynh J, Chand A, Gough D, et al. Therapeutically exploiting STAT3 activity in cancer—using tissue repair as a road map. *Nat Rev Cancer*. 2019;19(2):82—96.
50. Zhang M, Zhou L, Xu Y, et al. A STAT3 palmitoylation cycle promotes T_H17 differentiation and colitis. *Nature*. 2020;586(7829):434—439.
51. Dandawate P, Kaushik G, Ghosh C, et al. Diphenylbutylpiperidine antipsychotic drugs inhibit prolactin receptor signaling to reduce growth of pancreatic ductal adenocarcinoma in mice. *Gastroenterology*. 2020;158(5):1433—1449.
52. Heichler C, Scheibe K, Schmied A, et al. STAT3 activation through IL-6/IL-11 in cancer-associated fibroblasts promotes colorectal tumour development and correlates with poor prognosis. *Gut*. 2020;69(7):1269—1282.
53. Bharadwaj U, Kasembeli MM, Robinson P, et al. Targeting *Janus* kinases and signal transducer and activator of transcription 3 to treat inflammation, fibrosis, and cancer: rationale, progress, and caution. *Pharmacol Rev*. 2020;72(2):486—526.
54. Li T, Fu J, Zeng Z, et al. TIMER2.0 for analysis of tumor-infiltrating immune cells. *Nucleic Acids Res*. 2020;48(W1):W509—W514.
55. Li H, Chen L, Li JJ, et al. MiR-519a enhances chemosensitivity and promotes autophagy in glioblastoma by targeting STAT3/Bcl2 signaling pathway. *J Hematol Oncol*. 2018;11:70.
56. Xie Q, Yang Z, Huang X, et al. Ilamycin C induces apoptosis and inhibits migration and invasion in triple-negative breast cancer by suppressing IL-6/STAT3 pathway. *J Hematol Oncol*. 2019;12:60.
57. Zou S, Tong Q, Liu B, et al. Targeting STAT3 in cancer immunotherapy. *Mol Cancer*. 2020;19:145.
58. Bai L, Zhou H, Xu R, et al. A potent and selective small-molecule degrader of STAT3 achieves complete tumor regression *in vivo*. *Cancer Cell*. 2019;36(5):498—511.
59. Pore N, Wu S, Standifer N, et al. Resistance to durvalumab and durvalumab plus tremelimumab is associated with functional *STK11* mutations in patients with non-small cell lung cancer and is reversed by STAT3 knockdown. *Cancer Discov*. 2021;11(11):2828—2845.
60. Sun HJ, Xiong SP, Cao X, et al. Polysulfide-mediated sulfhydration of SIRT1 prevents diabetic nephropathy by suppressing phosphorylation and acetylation of p65 NF-κB and STAT3. *Redox Biol*. 2021;38:101813.
61. Kosack L, Wingelhofer B, Popa A, et al. The ERBB-STAT3 axis drives Tasmanian devil facial tumor disease. *Cancer Cell*. 2019;35(1):125—139.
62. Niu J, Sun Y, Chen B, et al. Fatty acids and cancer-amplified ZDHHC19 promote STAT3 activation through S-palmitoylation. *Nature*. 2019;573(7772):139—143.
63. Kim DN, Thiel BC, Mrozowich T, et al. Zinc-finger protein CNBP alters the 3-D structure of lncRNA Braveheart in solution. *Nat Commun*. 2020;11:148.
64. Pichler M, Rodriguez-Aguayo C, Nam SY, et al. Therapeutic potential of FLANC, a novel primate-specific long non-coding RNA in colorectal cancer. *Gut*. 2020;69(10):1818—1831.
65. Ichiba M, Nakajima K, Yamanaka Y, et al. Autoregulation of the *Stat3* gene through cooperation with a cAMP-responsive element-binding protein. *J Biol Chem*. 1998;273(11):6132—6138.

66. Yu Z, Cao W, Ren Y, et al. ATPase copper transporter A, negatively regulated by miR-148a-3p, contributes to cisplatin resistance in breast cancer cells. *Clin Transl Med*. 2020;10(1):57—73.
67. Karasic TB, O'Hara MH, Loaiza-Bonilla A, et al. Effect of gemcitabine and nab-paclitaxel with or without hydroxychloroquine on patients with advanced pancreatic cancer: a phase 2 randomized clinical trial. *JAMA Oncol*. 2019;5(7):993—998.
68. Martin M, Zielinski C, Ruiz-Borrego M, et al. Palbociclib in combination with endocrine therapy versus capecitabine in hormonal receptor-positive, human epidermal growth factor 2-negative, aromatase inhibitor-resistant metastatic breast cancer: a phase III randomised controlled trial—PEARL. *Ann Oncol*. 2021;32(4):488—499.
69. Wang T, Fahrmann JF, Lee H, et al. JAK/STAT3-regulated fatty acid β-oxidation is critical for breast cancer stem cell self-renewal and chemoresistance. *Cell Metabol*. 2018;27(1):136—150.
70. Xiang S, Dauchy RT, Hoffman AE, et al. Epigenetic inhibition of the tumor suppressor ARHI by light at night-induced circadian melatonin disruption mediates STAT3-driven paclitaxel resistance in breast cancer. *J Pineal Res*. 2019;67(2):e12586.